# Dietary phenolics and their microbial metabolites are poor inhibitors of trimethylamine oxidation to trimethylamine N-oxide by hepatic flavin monooxygenase 3

Lisard Iglesias-Carres[a], Sydney A. Chadwick-Corbin[a], Michael G. Sweet[a], Andrew P. Neilson[1a,b]*

[a]Plants for Human Health Institute, North Carolina State University, 600 Laureate Way, Kannapolis, Kannapolis, NC 28081, USA

[b]Department of Food, Bioprocessing, and Nutrition Sciences, North Carolina State University, 400 Dan Allen Drive, Raleigh, NC 27606, USA

***Corresponding author:** Dr. Andrew P. Neilson, Plants for Human Health Institute, 600 Laureate Way, Kannapolis, NC 28081, USA; email: aneilso@ncsu.edu; phone: +1-704-250-5495

**Running title:** chlorogenic acid does not inhibit FMO3 *in vitro*

Funding: Partial funding for this project was provided by the North Carolina Agricultural Research Service (NCARS) and the Hatch Program of the national Institute of Food and Agriculture (NIFA), U.S. Department of Agriculture. Funding sponsors had no role in study design; the collection, analysis and interpretation of data; in the writing of the report; and in the decision to submit the article for publication

**Keywords:** Atherosclerosis; Cardiovascular disease; FMO3; Trimathylamine; Trimathylamine N-oxide

## ABSTRACT

High circulating levels of trimethylamine N-oxide (TMAO) are a risk factor for development of cardiovascular disease. TMAO is formed through a microbiome-host pathway utilizing primarily dietary choline as a substrate. Specific gut microbiota transform choline into trimethylamine (TMA), and, when absorbed, host hepatic flavin-containing monooxygenase 3 (FMO3) oxidizes TMA into TMAO. Chlorogenic acid and its metabolites reduce microbial TMA production *in vitro*. However, little is known regarding the potential for chlorogenic acid and its bioavailable metabolites to inhibit the last step: hepatic conversion of TMA to TMAO. We developed a screening methodology to study FMO3-catalyzed production of TMAO from TMA. HepG2 cells were unable to oxidize TMA into TMAO due to their lack of FMO3 expression. Although Hepa-1 cells did express FMO3 when pre-treated with TMA and NADPH, they lacked enzymatic activity to produce TMAO. Rat hepatic microsomes contained active FMO3. Optimal reaction conditions were: 50 μM TMA, 0.2 mM NADPH and 33 μL microsomes/mL reaction. Methimazole (a known FMO3 inhibitor) at 200 μM effectively reduced FMO3-catalyzed conversion of TMA to TMAO. However, bioavailable chlorogenic acid metabolites did not generally inhibit FMO3 at physiological (1 μM) nor supra-physiological (50 μM) doses. Thus, the effects of chlorogenic acid in regulating TMAO levels *in vivo* are unlikely to occur through direct FMO3 enzyme inhibition. Potential effects on FMO3 expression remain unknown. Intestinal inhibition of TMA production and/or absorption are thus likely their primary mechanisms of action.



**Keywords:** Atherosclerosis; Cardiovascular disease; FMO3; Trimathylamine; Trimathylamine N-oxid

## 1. Introduction:

Cardiovascular disease (CVD) is one of the major causes of death worldwide [1]. A key factor in the development of CVD, cardiovascular risk and mortality is atherosclerosis [2]. In recent years, trimethylamine *N*-oxide (TMAO) has emerged as a novel, relevant biomarker and risk factor for the development of atherosclerosis, CVD and cardiovascular mortality [2–4]. Thus, controlling circulating levels of TMAO could have a significant benefit for public health.

TMAO is produced through a gut microbiota-host metabolic axis. First, choline is converted into trimethylamine (TMA) by specific gut bacteria with the choline utilization gene cluster *cutC/D*, encoding for TMA-lyases [5,6]. Other quaternary amines, such as L-carnitine and betaine can be converted into TMA by different enzymes as well [2,5,7]. Once TMA is formed in the gut, it can be absorbed by the host and reach the liver where flavin-containing monooxygenases (FMOs), particularly FMO3, oxidize it into TMAO [8–10]. Once in circulation, TMAO exerts several biological effects that ultimately contribute to atherosclerosis development and a higher risk of cardiovascular mortality [2,7,11].

Plant phytochemicals, and phenolic compounds in particular, have broadly been studied for their cardioprotective effects [12–14]. However, the mechanisms of this protection remain incompletely understood. In recent years, the ability of phenolics to modulate production of TMA and/or TMAO has emerged as another potential cardioprotective mechanism of action [7]. To explore this possibility, we recently screened and identified several phenolic compounds able to inhibit TMA production in an *ex vivo-in vitro* anaerobic colonic microbiota model [15,16]. One of the most potent inhibitors of TMA production in our model is chlorogenic acid. Further research performed by us and other authors also suggests the potential of chlorogenic acid for the modulation of circulating TMAO levels [15,17,18].

Native phenolics from the diet are generally poorly bioavailable, and a large percentage of the ingested dose reaches the colon where it is subjected to gut microbiota fermentation [19,20]. This makes the gut and gut microbiota an appealing target to study the role of phenolics as inhibitors of TMAO production via inhibiting choline metabolism to TMA by the microbiota[7]. However, a percentage of native phenolics and their gut-derived phenolic metabolites can also be absorbed by the host, and reach both the liver and systemic circulation [19,20]. Thus, inhibiting conversion of TMA to TMAO by hepatic FMO3 may also be a complementary mechanism for reducing TMAO producton *in vivo*. In some cases, the bioavailability of gut microbiota-metabolites is much higher

than the native compounds [21]. Of note, gut microbiota-derived phenolic metabolites have shown relevant bioactivities in various peripheral tissue models [21–23]. Furthermore, different phytochemicals have been shown to regulate circulating TMAO levels by reducing the gene expression and/or activity of FMO3 [24–29]. Thus, the aim of this study was to evaluate if bioavailable phenolic metabolites are able to inhibit the production of TMAO in the liver via direct inhibition of FMO3. To achieve this, three different *in vitro* screening models were developed and evaluated: human hepatic cells (HepG2), mouse hepatic cells (Hepa-1), and rat hepatic microsomes.

## 2. Materials and methods:

### 2.1. Chemicals and reagents:

Ammonium formate, ammonia, ethyl bromoacetate, TMA, TMA-$^{13}C_3$-$^{15}N$, TMAO, TMAO-$d_9$, 3-(4,5-dimethylthiazol-2-yl)-2,5-diphenyl tetrazolium bromide (MTT reagent), DMSO, NADPH, hepatic microsomes from female Sprague-Dawley rats, quinic acid, chlorogenic acid, caffeic acid, ferulic acid, isoferulic acid, dihydrocaffeic acid, dihydroferulic acid, dihydroisoferulic acid, *p*-coumaric acid, *m*-coumaric acid and methzimazole (MTM) were purchased from Sigma-Aldrich/Millipore (St. Louis, MO, USA). Acetonitrile and water (HPLC grade) were purchased from VWR International (Suwanee, GA, USA). HepG2 and Hepa-1c1c7 (Hepa-1) cells were purchased from ATCC (Manassas, VA, USA). Dulbecco's Modified Essential Media (DMEM), nucleoside-free α-minimal essential medium (MEM-α), non-essential amino acids (NEAA), penicillin, streptomycin and gentamicin were purchased from Lonza (Morristown, NJ, USA). Heat-inactivated fetal bovine serum (FBS) was purchased from R&D systems (Minneapolis, MN, USA). HEPES was purchased from Fisher Scientific (Waltham, MA, USA)

### 2.2. General cell culture:

HepG2 (human hepatocyte) cells were cultured in growth media consisting of DMEM, 10 % FBS, 0.5 % penicillin/streptomycin, 0.1 % gentamicin, and 1 % NEAA. Cells were maintained at incubator conditions of 37 °C in a 5 % $CO_2$/air with 90 % humidity. Growth medium was changed every 2 days, and cells were sub-cultivated 1 – 2 times a week. Subcultivation and treatments were only performed to cells that reached > 80 % confluence. Hepa-1 cell culture followed the same procedure, but grown in MEM-α with 10 % FBS, 1% HEPES, 0.5 % penicillin/streptomycin, 0.1 % gentamicin, and 1 % NEAA.

### 2.3. Screening method in human hepatic cells:

122 ***2.3.1. TMA toxicity in HepG2:***

123 A first set of experiments was performed in HepG2 cells to evaluate potential TMA toxicity. 48 h
124 prior to treatments, cells were seeded at $3.5x10^5$ cells/mL in 24-well plates with 1 mL of growth
125 media. The day of the experiment, growth media was removed and cells were washed once with
126 pre-warmed PBS 1X. Cells were then treated with 950 µL DMEM and 50 µL TMA for final TMA
127 concentrations of 10 – 200 µM. A control without TMA was achieved by treating cells with 950 µL
128 DMEM and 50 µL PBS. Cells were exposed to experimental conditions for 10 h, and toxicity (loss
129 of viability) was assessed via the MTT assay.

130

131 ***2.3.2. TMAO production in HepG2:***

132 A second set of experiments was performed in HepG2 cells to evaluate their capacity to produce
133 TMAO. 48 h prior to the treatments, cells were seeded as described above in 24-well plates. 24
134 h prior to treatment, cells were pre-treated with 100 µM TMA in growth media. The day of the
135 experiment, media was removed and cells were washed once with pre-warmed PBS. Cells were
136 then treated with ± 100 µM TMA and ± NADPH (0 – 40 mM) in DMEM. Toxicity controls included
137 TMA and NADPH-free conditions, and NADPH-free conditions. To assess spontaneous chemical
138 (non-cellular) production of TMAO, cell-free controls with 100 µM TMA and 0 or 2 mM NADPH
139 were included. At selected time points (0, 1.5, 3, 4.5, 6, 7.5, 9, 10.5 and 24 h), aliquots (75 µL) of
140 treatment media were taken, immediately mixed with equal volume of acetonitrile and frozen until
141 TMA and TMAO analyses. At the end of the kinetic study (24 h), all treatments (except cell-free
142 controls) were subjected to cytotoxic evaluation by MTT assay.

143

144 **2.4. Screening method in Hepa-1 cells:**

145 Due to the lack of observed TMAO production in HepG2, we next investigated the potential of
146 Hepa-1 (rat hepatocyte) cells as a alternative *in vitro* cell model for TMAO production due to their
147 previously reported FMO activity [30]. 48 h prior to the treatments, cells were seeded as described
148 above in 24-well plates. 24 h prior to treatment, cells were pre-treated with 100 µM TMA in growth
149 media. The day of the experiment, media was removed and cells were washed once with pre-
150 warmed PBS. Cells were then treated TMA (0 – 100 µM) and NADPH ( 0.0 – 2 mM) in MEM-α or
151 complete growth media. A batch of experiments with the same TMA and NADPH treatments
152 concentrations were performed in Hepa-1 cells, but without TMA pretreatment. None of these
153 non-pretreatment conditions reported TMAO production (data not shown). At time 0 h and 24 h
154 aliquots (100 µL) of treatment media were taken, immediately mixed with an equal volume of
155 acetonitrile and frozen until TMA and TMAO analyses.

156

157 ***2.5. Toxicity assessment in cell lines:***

158 Potential cytotoxic effects of treatments on cells were evaluated through the MTT assay [15]. At
159 the end of the kinetic studies, remaining treatment media was removed and cells washed with 1
160 mL PBS. Cells were then treated with 200 µL DMEM (HepG2) or MEM-α (Hepa-1) supplemented
161 with 0.5 mg/mL MTT reagent. After incubation at 37 °C for 20 min, media was aspirated and 1 mL
162 DMSO was added and shaken until reduced MTT crystals were solubilized. An aliquot of 100 µL
163 was read at 560 nm in a SpecraMax iD3 plate reader (Molecular Devices, San Jose, CA, USA).
164 Results were relativized to control conditions, and expressed as a percentage of change against
165 control (untreated cells) ± SEM (*n*=3).

166

167 **2.6. Screening method in microsomes:**

168 A rat microsome-based screening method was developed to evaluate the potential of bioavailable
169 phenolics and their microbial metabolites to inhibit FMO3-catalyzed TMAO formation. Microsome
170 assays were conducted in phosphate buffer (pH 7.4) in a water bath at 37 °C. Different
171 concentrations of microsomes (0 – 200 µL/mL reaction), TMA (0 – 50 µM) and NADPH (0 – 4
172 mM), and reaction times (0-45 min) were studied to optimize the assay. Further, MTM (a known
173 FMO3 enzyme inhibitor) was evaluated 0 – 1 mM. Quinic acid, chlorogenic acid, caffeic acid,
174 ferulic acid, isoferulic acid, dihydrocaffeic acid, dihydroferulic acid, dihydroisoferulic acid, *p*-
175 coumaric acid and *m*-coumaric acid were used as representative bioavailable metabolites of
176 chlorogenic acid [14] and evaluated as TMAO production inhibitors at a physiologically relevant
177 dose (1 µM), as well as a pharmacological dose (50 µM). At selected timepoints (0 – 45 min),
178 reaction aliquots (25 – 50 µL) were collected and mixed with ice-cold acetonitrile. Then, samples
179 were filtered through a AcroprepAdv 0.2 µm WWPTFE 96-well filtering plates (Pall Corporation,
180 Port Washington, NY, USA) by centrifugation (10 min, 3,400 x g), collected in a fresh 96-well
181 collection plate and frozen at –80 °C until extraction/derivatization with an OT-2 liquid handler
182 robot (Opentrons, NY, USA).

183

184 **2.7. Extraction and quantification of TMA and TMAO.**

185 Extraction and quantification of TMA and TMAO from cell culture and microsome reaction
186 supernatants were carried out as described by Iglesias-Carres *et al*. [15]. To extract TMAO, 25
187 µL of sample:acetonitrile mixture (50:50; v:v) were mixed with 10 µL of $ZnSO_4$ (5 % w/v in water),
188 100 µL acetonitrile and 20 µL TMAO-$d_9$ [internal standard (IS); 5 µM] in 96-well plates. After
189 sonication for 5 min in a water bath, samples were filtered through AcroprepAdv 0.2 µm WWPTFE

190 96-well filtering plates (Pall Corporation, Port Washington, NY, USA) by centrifugation (10 min,
191 3,400 x g), collected in a fresh 96-well collection plate and frozen at –80 °C until UHPLC-MS/MS
192 analysis. TMA requires derivatization to ethyl betaine to facilitate LC-MS/MS ionization. Briefly,
193 25 µL of cell supernatant:acetonitrile (50:50; v:v) were mixed with 20 µL of TMA-$^{13}C_3$-$^{15}N$ IS
194 solution (5 µM), 8 µL concentrated ammonia and 120 µL ethyl bromoacetate (20 mg/mL), and let
195 sit for 30 min. Then, 120 µL 50 % acetonitrile/0.025 % formic acid in distilled water were added.
196 Samples were then filtered and stored as described above. Sample and reagent plating were
197 performed using an OT-2 liquid handler (Opentrons, NY, USA).
198
199 After extraction, analytes were analyzed via UPLC-ES-MS/MS. TMAO and TMA were analyzed
200 separately, but with the same UHPLC-ESI-MS/MS method employing distinct MS/MS transitions.
201 Briefly, separation was achieved on a Waters Acquity UPLC (Milford, MA, USA) with an ACQUITY
202 BHE HILIC column (1.7 µm, 2.1x100 mm) coupled to an ACQUITY BHE HILIC pre-column (1.7
203 µm, 2.1x5 mm). Mobile phases were 5 mM ammonium formate in water (pH 3.5) (A) and
204 acetonitrile (B). The gradient was isocratic (80 % B) for 2 min, with a flow rate of 0.65 mL/min.
205 Colum temperature was 30 °C, and autosampler at 10 °C. Quantification was achieved by
206 coupling UPLC with a Waters Acquity triple quadrupole mass spectrometer. Source and capillary
207 temperatures were 150 and 400 °C, respectively. Capillary voltage was 0.60 kV, and desolvation
208 and cone gas flows (both $N_2$) were 800 and 20 L/h, respectively. Electrospray ionization (ESI)
209 was operated in positive mode, and data were acquired by multiple reaction monitoring (MRM) in
210 MS/MS mode. Multi-reaction monitoring (MRM) fragmentation conditions of analytes and IS
211 compounds can be found in **Table S1**.
212
213 For quantification, HPLC water was spiked with 0 – 200 µM TMA and TMAO standards to obtain
214 external calibration curves. Samples were quantified by interpolating analyte/IS peak abundance
215 ratios in the standard curves. Data acquisition was carried out using Masslynx software (V4.1
216 version, Waters). Method sensitivity was determined by limit of detection (LOD) and limit of
217 quantification (LOQ), respectively defined as the concentration of analyte corresponding to 3 and
218 10 times the signal/noise ratio. LOD and LOQ show the lowest concentration required to be
219 injected (5 µL) for analyte detection and quantification. Method detection limit (MDL) and method
220 quantification limits (MQL), respectively defined as the concentration of analyte corresponding to
221 3 and 10 times the signal/noise ratio, represent the minimum concentration of analytes in cell
222 supernatant samples to be detected and quantified. Working linearity range concentrations also

223 refer to concentrations of standards on the volumes added to the extraction/derivatization
224 procedure. These method quality parameters can be found in **Table S2**.
225
226 **2.8. FMO3 quantification:**
227 FMO3 protein content/presence was evaluated in HepG2, Hepa-1 and rat microsomes. HepG2
228 were cultured as described above in T25 flasks with or without TMA (50 μM) and NADPH (0.2
229 mM) for 24 h in triplicates. Hepa-1 followed the same treatments, but with complete media instead
230 of DMEM. Cells were washed twice with PBS, scraped off in 3mL of PBS and collected in 15mL
231 centrifuge tubes. Cells were then centrifuged (5 min, 800 rpm) andreconstituted in 1 mL fresh
232 PBS. Cells were washed twice with 5 mL PBS by centrifgugation and resuspension, and
233 reconstituted in 1 mL fresh PBS. Cell suspensions and microsomes were lysed with1:1 (v:v) RIPA
234 with 5 min sonication in a water bath, centrifuged (10 min, 3,400 x g, 4 °C) and supernantants
235 collected and frozen at – 80 °C until analyses. FMO3 protein content was evaluated by species-
236 specific ELISAs (MyBioSource, San Diego, CA, USA) per kit instructions: mouse-specific FMO3
237 (kit MBS9327471) for Hepa-1 cells, rat-specific FMO3 (kit MBS9901107) for rat microsomes, and
238 human-specific FMO3 (MBS9901102) for HepG2 cells. Pierce BCA protein assay kit (Thermo
239 Scientific, Rockford, IL, USA) was used for total protein quantification of homogenates used for
240 ELISAs. Results were expressed as μg FMO3/mg protein ± SEM ($n$=3).
241
242 **2.9. Statistics.**
243 Prism 8.0 (GraphPad, La Jolla, CA, USA) was used for statistical analyses and graphing. In all
244 cases, statistical significance was defined *a prioi* as $p<0.05$. Specific statistical tests employed
245 varied based on experimental design, and are stated in the caption for each graph.
246
247 **3. Results:**
248 **3.1. TMA and NADPH toxicity on HepG2 cells.**
249 We first evaluated if TMA concentrations between 10 – 200 μM were toxic to HepG2 cells in order
250 to determine the maximum concentration that could be used in the assay while maintaining viable
251 cells. No significant changes in cell respiration (MTT) were reported between concentrations after
252 10 h TMA exposure (Fig. 1A), suggesting TMA concentrations up to 200 μM are not toxic to
253 HepG2 cells. Next, HepG2, cells were pre-treated with 100 μM TMA 24 h prior to treatment with
254 100 μM TMA and a range of NADPH concentrations (**Fig. 1B**). Despite a few statistically
255 significant differences, co-treatment with TMA 100 μM and different concentrations of NADPH in
256 HepG2 did not change cell respiration more than 20% compared to untreated cells. Our results

257 show an inverse “U-shaped” or hormetic effect of NADPH on cell respiration, suggesting that an
258 optimal viability of cells is obtained at NADPH concentrations of 0.2 mM when co-treated with
259 TMA 100 μM.
260
261 **3.2. TMA stability and lack of TMAO production in HepG2 culture:**
262 To eliminate the possibility that TMAO was produced by a non-cell catalyzed reaction in our assay,
263 different conditions were evaluated (**Fig. 2A**). In cell-free conditions (red bars) with 100 μM TMA
264 and 2 mM NADPH (highest concentration tested), TMA was stable and its concentrations did not
265 decrease over time. Similar results were reported when neither HepG2 cells nor NADPH were
266 present in the mixture (blue bar). TMAO was not detected in any of the cell-free conditions. When
267 HepG2 were treated for 24 with 100 μM TMA and 2 mM NADPH, TMA levels still did not decrease
268 (black bars), nor was TMAO detected. The full 24 h kinetic plot of TMA in these epxperimental
269 conditions can be found in the form of absolute values in **Figure S1A**, and in the form of
270 percentage against control in **Figure S1B**. This lack of production of TMAO (data not shown) and
271 degradation/use of TMA (**Fig. 2B**) was also reported in HepG2 cells co-treated with TMA 100 μM
272 and NADPH 0 - 2 mM. The full 24 h kinetic plot of TMA in these epxperimental conditions can be
273 found in the form of absolute values in **Figure S2A**, and in the form of percentage against control
274 in **Figure S2B**. Additionally, TMA was also not produced in our first trial (no pre-treatment with
275 TMA nor co-treatment with NADPH) with HepG2 over 10 h (data not shown). Overall, our results
276 show that TMA is not spontaneously chemically degraded nor converted into TMAO in our
277 experimental design in the absence of cells, and that HepG2 are also not capable of transforming
278 TMA into TMAO (likely due to lack of FMO3).
279
280
281 **3.3. Lack of TMAO production in Hepa-1 cell cultures:**
282 Given the lack of TMAO production in human HepG2 cells, we next evaluated mouse Hepa-1
283 cells as another potential TMAO-producing cell model due to previously reported FMO activity of
284 this cell line towards other FMO substrates [30]. The lack of toxicity and TMA degradation in the
285 HepG2 assays was used to design the approach in Hepa-1 cells. Hepa-1 cells were pre-treated
286 with 100 μM TMA for 24 h before the kinetic experiment to promote FMO3 gene expression and
287 activity. The initial (0h) and final (24h) concnetrations of TMA on pre-treated Hepa-1 cells co-
288 exposed to 10 – 100 μM TMA and 1 mM NADPH were fairily constant (**Fig. 3A**), while TMAO was
289 not detected at 0 or 24 h. Of note, background (no TMA and no NADPH) as well as 0 μM TMA
290 treatments resulted in initial and final TMA concentrations around 7 μM and 11 μM, respectively.

291 This is most likely due to remaining TMA from pre-treatment. Simmilarly, pre-treated Hepa-1 cells
292 co-exposed to 0.2 – 2 mM NADPH and 50 μM TMA reported a slight decrease of TMA over 24h,
293 and a lack of production of TMAO (**Fig. 3B**). In this case, background (no TMA and no NADPH)
294 was the same condition as before, and NADPH 0 mM reported a similar TMA behaviour as +
295 NADPH conditions. Overall, our results indicate that TMA is not being metabolized into TMAO by
296 Hepa-1 cells within 24 h. All these conditions were performed in MEM-α media. We then evaluated
297 if the use of complete growth media would substantially alter TMAO production. **Figure 3C** shows
298 that Hepa-1 cells pre-treated and non-pretreated with TMA are unable to metabolize TMA into
299 TMAO when co-cultured with TMA 50 μM and NADPH 1 mM for 24h. Although cell toxicity (MTT)
300 data is not reported, cells cultured with complete media reported a higher mitochondrial
301 respiration of those cultured with MEM-α, regardless of pre-treatment or non-pretreatmet with
302 TMA. Taken together, our data shows that Hepa-1 cells are also not an appropriate model in
303 which to study TMAO formation.
304
305 **3.4. Validation of microsomal production of TMAO:**
306 After ruling out HepG2 and Hepa-1 cell lines, we evaluated rat liver microsomes as a potential
307 model. Microsomes from female rats were selected based on previous findings that female rats
308 typically have greater FMO3 expression/activity compared to male rats and either sex of mouse
309 [31–34]. To validate our method, we again evaluated if TMA was stable in our experimental
310 conditions and that it was not oxidized into TMAO by a non-enzymatic catalyzed reaction. To do
311 so, we performed reactions with or without microsomes (100 μL/mL), TMA (10 μM) and/or NADPH
312 (2 mM), as well as 2X these concentrations. Samples were collected at 15 and 30 min (**Fig. 4**).
313 Our results show that the buffer does not contain TMA, and TMAO is not formed in the absence
314 of microsomes. Similarly, microsomes (background, no TMA added) do not supply TMA, and thus
315 TMAO is not formed. This shows that all TMA in our assay is exogenously added, and that all
316 TMAO formed comes from exogenously-added TMA via the microsomnes. We also showed that
317 TMAO is only formed when microsomes and TMA are incubated with NADPH. When no NADPH
318 is added, TMA remains stable and TMAO is not produced. Thus, microsomes, TMA and NADPH
319 are all required factors in the assay. Our data also shows that the reaction is fast: at 15 min all
320 TMA is consumed and converted into TMAO. This is also true when 2 X NADPH (4 mM) and 2 x
321 microsomes (200 μL/mL) are added to the mixture. Finally, our data also demonstrates that
322 NADPH does not spontaneously oxidize TMA into TMAO, and that microsomes are required for
323 the formation of TMAO. Overall, this preliminary assay suggests that 1) rat liver microsomes are
324 a valid model for TMA coinversion to TMAO, and 2) there is no TMA and TMAO contribution of

325 the microsomes and other reagents of the assay; 3) TMAO is only formed when TMA, NADPH
326 and microsomes are co-incubated; and 4) lower concentrations of NADPH and microsomes
327 should be used in further studies in order to capture the kinetics of this reaction.
328
329 Once our rat liver microsome method was validated as a model of TMA conversion to TMAO, we
330 sought to define appropriate TMA concentrations and characterize the kinetics of the microsomal
331 reaction. Due to the results of our preliminary assay, reactions were conducted at a final
332 concentration of 33 μL/mL microsomes, with 1 mM NADPH. TMA was tested at 0, 20 and 50 μM
333 (**Fig. 5**). Although the quantified concentrations were higher than anticipated based on
334 calculations, our data shows that adding 20 μM TMA (quantified at 29.01 μM at 1 min) was almost
335 completely consumed by 30 min, while when adding 50 μM TMA (quantified at 64.94 μM at 1 min)
336 a significant amount of TMA was still present at 30 min (28.32 μM). Thus, adding 20 μM TMA was
337 selected for further studies. Overall, our selected conditions were 33 μL/mL microsomes, 1 mM
338 NADPH and 20 μM TMA.
339
340 Finally, we evaluated the inhibitory potential of MTM, a known FMO3 competitive inhibitor, in our
341 microsome system. MTM was tested at 20 – 1000 μM, while other experimental conditions were
342 fixed at 20 μM TMA, 1 mM NADPH and 33 μL/mL microsomes. A background (no TMA and no
343 MTM) condition was included too. Our results corroborated that MTM at concentrations ≥ 50 μM
344 were able to inhibit TMA use and TMAO production ($p<0.05$ by Two-Way ANOVA, main effects:
345 treatment, time; effect of treatment assessed by Tukey's *post hoc* test) compared to inhibitor-free
346 conditions (**Fig. 6**). However, when Sidak's *post hoc* test was applied to evaluate the differences
347 at individual time points between inhibitor-free and MTM-supplemented conditions, only
348 concentrations ≥ 200 μM MTM reported relevant statistically-significant changes (**Fig. S3**). Thus,
349 MTM 200 μM was selected as a positive control for further experiments.
350
351 **3.5. Chlorogenic acid and related compounds do not inhibit FMO3 activity**
352 Once our TMAO inhibition assay method was defined and MTM optimized, we next screened for
353 FMO3 inhibitory effects of different chlorogenic acid-related molecules at a physiologically
354 relevant dose of 1 μM. Overall, few of the selected compounds significantly inhibitted TMA use
355 and TMAO production. No treatment other than MTM produced a kinetic curve of TMA use
356 statistically different (overall main effect of treatment by Two-Way ANOVA) from the inhibitor-free
357 control (**Fig. 7A**). The metabolite dihydrocaffeic acid (DHC) was the only compound besides MTM
358 to present a TMAO kinetic curve statistically different from the control (overall main effect of

359 treatment by Two-Way ANOVA, **Fig. 7B**). However, when the AUCs of TMA were analyzed
360 (reflecting total TMA use over time), isoferulic and *p*-coumaric acids (along with MTM) reported
361 statistically significant TMA increases (i.e reduced TMA use) compared to control conditions,
362 suggesting that they inhibited TMA use (**Fig. 7C**). Nevertheless, only DHC (along with MTM) was
363 able to statistically reduce the AUC of TMAO, which agrees with the effects observed in the kinetic
364 curves (**Fig. 7D**). Of note, quinic acid, isoferulic and DHC statistically reduced TMAO percentage
365 against control conditions, while no compound did the same for TMA percentage (**Fig. S4**).
366
367 In order to determine whether higher concentrations would produce inhibition, we evaluated a
368 supraphysiological (pharmacological) dose of 50 μM only obtainable by injection. No compound
369 inhibited the use of TMA at 50 μM. Rather, *p*-coumaric acid and *m*-coumaric acid actually increase
370 production of TMAO , expressed as percentage of change against control conditions (**Fig. S5**).
371 Overall, our data suggests that chlorogenic acid and its related compounds generally are likely to
372 exert a small or no inhibitory effects on TMA conversion to TMAO by FMO3.
373
374 **3.6. FMO3 levels in HepG2, Hepa-1 and rat microsomes**
375 Finally, to further validate our results, levels of FMO3 in the models used were evaluated using
376 species-specific FMO3 ELISA kits (**Fig. 8**). Of note, HepG2 cells, either treated with or without
377 TMA 50 μM and NADPH 0.2 mM, did not report any levels of FMO3 detectable by human FMO3-
378 specific ELISA. On the other hand, Hepa-1 cells reported high levels of FMO3 detectable by the
379 mouse FMO3-specific ELISA after pre-treatment with TMA 50 μM and NADPH 0.2 mM, but their
380 levels were not detected without this pre-treatment. The lack of FMO3 content in HepG2 aligns
381 with the lack of TMAO formation in that model. Interestingly, much greater levels of FMO3 were
382 detected in mouse Hepa-1 cells compared to rat microsomes, although Hepa-1 were unable to
383 produce TMAO and microsomes showed great efficiency to do so.
384
385 **4. Discussion:**
386 Cardiovascular disease-related deaths account for 31% of all deaths worldwide [1]. Recently,
387 increased circulating levels of TMAO were shown to promote atherosclerosis development and
388 identified as a risk factor for CVD [2–4]. There is a need for complementary strategies to reduce
389 cardiovascular dicsease burden worldwide. Several phytochemicals, including phenolic
390 compounds, have been shown to inhibit TMAO production through targeting the gut microbiota
391 [7]. We have recently identified several phenolic compounds, such as chlorogenic acid and
392 epicatechin, as potential bioactive compounds to manage TMAO levels by inhibiting microbial

393 production of TMA [15–17]. However, TMA conversion to TMAO is the second step in this
394 metabolic pathway, and it is possible that these compounds could achieve their cardioprotective
395 effects by inhibiting the catalytic activity of FMO3, as reported in previous studies of other
396 phytochemicals [7]. We thus aimed to develop an *in vitro* screening method to evaluate the
397 potential of bioavailable phenolic metabolites to inhibit FMO3-catalyzed conversion of TMA to
398 TMAO in the liver. To achieve this, we employed human hepatic cells (HepG2), mouse hepatic
399 cells (Hepa-1), and rat hepatic microsomes.
400
401 Firstly, we tried to develop a TMAO inhibition method through the use of HepG2, a convenient
402 and widely used hepatocyte human cell model. HepG2 is an immortalized, commercially-available
403 hepatic cell line isolated from a hepatocellular carcinoma from a 15-year-old white male [35]. Our
404 results showed that concentrations of TMA as high as 200 μM were not toxic to HepG2 cells (**Fig.**
405 **1A**). However, HepG2 cells were unable to transform TMA into TMAO. In order to attempt to
406 stimulate the production of TMAO, we pre-treated HepG2 cells with 100 μM for 24 h. FMO3 is a
407 FAD- and a NADPH-dependent enzyme [9]. Thus, after pre-treatment, HepG2 cells were treated
408 with TMA 200 μM and a range of NADPH concentrations from 0 – 2 mM for 24 h. Pre-treatment
409 with TMA and co-treatment with TMA and NADPH was generally not toxic for HepG2 cells (**Fig.**
410 **1B**). FMOs are generally thought to be a non-inducible family of genes, although several
411 compounds can increase their gene expression but not their protein content and activity [36]. Pre-
412 treatment with TMA and co-treatment with TMA and NADPH was insufficient to promote HepG2
413 catalytic conversion of TMA into TMAO (**Fig. 2B**). Previous studies in HepG2 cells have reported
414 FMO activity against different substrates, but not TMA [37]. However, other authors have shown
415 that although the FMO3 gene is present in HepG2 cells, HepG2 cells are unable to express FMO3
416 protein [38,39]. When the levels of FMO3 were analysed in lysed cells, FMO3 was not detected
417 (**Fig. 8**). Although the ELISA kit used was not specific to cell clutures, our results agree with the
418 lack of expression of FMO3 reported by others in the literature. To our knowledge, this is the first
419 attempt to develop a FMO3 inhibition method using non-transfected hepatic cells. We have shown
420 that human-derived HepG2 cells are not a good model for our purposes, attributed to their lack of
421 FMO3 expression.
422
423 Our second attempt to model FMO3 inhibition (enzme activity, gene expression and/or protein
424 content) was to reproduce our HepG2 approach in a mouse-derived hepatic cell line: Hepa-1.
425 Hepa-1 cells, derived from *Mus musculus* hepatoma, have been previously shown to express the
426 FMO3 gene and possess activity against ethionamide [36]. Thus, Hepa-1 cells were selected to

427 further develop our screening method. Hepa-1 cells were pre-treated with 100 μM TMA for 24 h,
428 and then treated with different concentraions of TMA (0 – 100 μM) and NADPH (0 – 2 mM). Similar
429 to HepG2, Hepa-1 cells were unable to metabolize TMA into TMAO (**Fig. 3A-B**) in MEM-α.
430 Although cell respiration increased when cultured with complete growth media (data not shown),
431 these cells wee unable to produce TMAO when co-treated with TMA 50 μM and NADPH 1 mM
432 (**Fig. 3C**), regardless of pre-treatment with TMA or not. Interestingly, we reported that Hepa-1
433 cells do express significant levels of some form of FMO3 (detectable by mouse-specific FMO3
434 ELISA) when pre-treated with TMA 50 μM and NADPH 0.2 mM (**Fig. 8**), albeit with significant
435 inter-sample variability (3 indvidual cell culture flasks were grown up for this assay and analyzed
436 separately). However, this was apparently insufficient for production of TMAO, which indicates
437 that Hepa-1 cells are also not a good model to study FMO3 inhibiton. This was somewhat
438 unexpected, especially when compared to detected FMO3 levels in rat microsomes, an efficient
439 model of TMAO production as per our data. A relevant factor to consider is that our results are
440 relative to the protein content of our samples. Microsomes were much richer in total protein than
441 our Hepa-1 cell lysates (data not shown), and normalization to total protein thus lowered the
442 relative levels of FMO3 compared to Hepa-1 cell lysates. Furthermore, the ELISA kits used to
443 perform these assays were not specific for cells (or microsomes for that matter) and the variability
444 in detected mouse Fmo3 was high. Thus, FMO3 levels should not be directly compared between
445 these models. Rather, this data should be interpreted as a indicator of presence (or lack of) FMO3
446 in our models. Finally, is important to note that ELISA detection of a specific antigen and full
447 catalytic activity are not synonymous, and the Hepa-1 cells are not a useful model for studying
448 TMA conversion to TMAO despite high levels of ELISA-detectable FMO3.Overall, our results
449 suggest that although cultured Hepa-1 cells express some form f FMO3, this enzyme is not
450 capable of significant conversion of TMA to TMAO.
451
452 Overall, our results in immortalized and commercially-available human (HepG2) and mouse
453 (Hepa-1) cell lines highlight the lack of ability of these cell lines to produce TMAO. To our
454 knowledge, although other FMO3 and FMO substrates may be metabolized by these cell lines,
455 this is the first study to attempt to assess whether or not these cell lines are able to metabolize
456 TMA into TMAO. Potentially, primary hepatic cell cultures could be used to this aim, but not Hepa-
457 1 and HepG2 cells. Noteworthily, this suggests that the study of compounds that can inhibit FMO3
458 TMAO production should be conducted in other *in vitro* models (*i.e.,* hepatic microsomes) or *in*
459 *vivo*. While microsomes may provide insights into direct FMO3 enzme inhibitions of chlorogenic

460 acid derived compunds, other mechanisms of actions, such as effects on gene expression and/or
461 protein content regulation, may only be evaluated *in vivo* or in primary hepatocytes [7].
462
463 Finally, we aimed to develop a rat microsome screening method that would convert TMA to TMAO
464 and thus allow the identification of direct FMO3 enzyme inhibitors. In this case, female rat
465 microsomes presented a concentration of FMO3 of 0.29 ng FMO3/mg protein (**Fig. 8**), which was
466 much lower compared to that of Hepa-1 cells (27.32 ng FMO3/mg protein). Despite that, these
467 microsomes presented FMO3 activity (**Fig. 4**), which was not the case of Hepa-1. The FMO3
468 activity in microsomes allowed the development of our methodology. Our initial method validity
469 assays demonstrated that TMA and NADPH need to be present in microsome preparations for
470 TMAO to be formed. The absence of either or both results in a lack of TMAO production (**Fig. 4**).
471 Further, we demonstrated that TMA is stable under our experimental conditions and only oxidized
472 into TMAO with the presence of both microsomes and NADPH. By further optimizing TMA,
473 NADPH and microsomes concentration, we defined our optimized method conditions at a
474 concentration of 20 μM TMA, 33 μL/mL microsomes, 1 mM NADPH and 45 min reaction time
475 (**Fig. 5**). To compare the effects of tretaments (*i.e.,* bioavailable phenolic metabolites) to a positive
476 control (*i.e.,* known FMO3 enzyme inhibitor) we optimized the concentrations of MTM. Results
477 showed that MTM at 200 μM achieved a TMAO production and TMA use inhibition (**Fig. 6** & **Fig.**
478 **S3**), and thus this concentration of MTM was used in further experiments.
479
480 Once our microsomes method was optimized, we evaluated the potential of bioavailable
481 chlorogenic acid metabolites as FMO3 inhibitors (**Fig. 7** & **Fig. S4**) at a physiologically-relevant
482 dose of 1 μM that can be achieved in circulation [14,40]. We selected quinic acid, chlorogenic
483 acid, caffeic acid, ferulic acid, isoferulic acid, dihydrocaffeic acid, dihydroferulic acid,
484 dihydroisoferulic acid, *p*-coumaric acid and *m*-coumaric acid. These compounds are structurally
485 related to chlorogenic acid (**Fig. S6**), and are formed during digestion and/or microbial action on
486 chlorogenic acid. In humans, ~1/3 of the ingested dose of chlorogenic acid in foods can be
487 absorbed throughout the gastrointestinal tract in its intact, unmetabolized form. About 7% of the
488 ingested dose of chlorogenic acid can be hydrolized in the small intestine into caffeic acid
489 (phenolic moiety) and quinic acid (non-phenolic meoiety), and then absorbed. The remaining
490 chlorogenic acid can reach the colon, where it is fermented by the gut microbiota into
491 dihydrocaffeic acid (reduction of double bond in side chain) as well as smaller phenolic acid
492 derivates. Caffeic and dihydrocaffeic acids can also be absorbed and undergo phase-II
493 metabolism in the gut epithelia and liver through the catalytic activity of catechol O-methyl

494 transferase (COMT). This generates ferulic and isoferulic acids (positional isomers), and its
495 reduced froms dihydroferulic and dihydroisoferulic acids [14]. Thus, these compounds could all
496 be found in circulation following chlorogenic acid consumption. After the consumption of a
497 decaffeinated green coffee beverage rich in chlorogenic acid and related compounds, the
498 maximum concentration in human plasma of the most bioavailable quantified compound were of
499 5.9 ± 4.2 μM chlorogenic acid, and of 0.4 ± 0.03 μM *p*-coumaric acid for the least bioavailable
500 quantified metabolite [40].
501
502 It is important to highlight that targeting FMO3 inhibition in humans should be conducted with
503 caution, as a strong inhibition of this enzyme could lead to trimethylaminuria or "fish-odor
504 syndrome" (increased levels of circulating TMA), which generates severe psychosocial problems
505 related to the excretion of TMA through sweat, breath and urine [41]. However, this is unlikely, as
506 consumption of phytochemicals has not been previously reported to cause trimethylaminuria.
507 Overall, bioavailable metabolites of chlorogenic acid did not have a dramatic effect on TMA use
508 or TMAO production. Rather, results were very subtle. The only compound able to modulate the
509 kinetic curve of TMAO formation was dihydrocaffeic acid, while none did that for the curve of TMA
510 (**Fig. 7A – B**). This effect was translated into a higher AUC of TMAO compared to control
511 conditions (**Fig. 7D**). Surprisingly, the AUC of TMA for reactions with 1 μM of isoferulic acid and
512 *p*-comaric acid was higher than control conditions, suggesting that these compounds prevented
513 TMA use, but not TMAO production. When results were epressed as percentage of change
514 against control conditions (**Fig. S4**), quinic acid (the non-phenolic part of chlorogenic acid), ferulic
515 acid and dihydrocaffeic acid were able to reduce TMAO % production against control conditions.
516 Our data suggests that dihydrocaffeic acid could play a small role in the inhibition of *in vivo* TMAO
517 formation of chlorogenic acid through a direct enzyme inhibition [18].
518
519 To further validate that bioavailable phenolic metabolites from chlorogenic acid do not or very
520 poorly inhibit FMO3 production of TMAO, the selected metabolites were tested in our assay at a
521 pharmacological dose of 50 μM (**Fig. S5**), impossible to achieve through the diet. Although this is
522 an approach with no relevance to dietary intake, it can be useful to determine whether or not these
523 compounds could potentially inhibit TMAO formation at any dose. A lack of bioactivity at these
524 high doses virtually guarantees the lack of bioactivity at physiologically-relevant doses. Our
525 results show that at these high concentrations, phenolic compounds still do not inhibit the use of
526 TMA (expressed as percentage against control conditions). However, *p*-coumaric and *m*-
527 coumaric acid enhanced the production of TMAO (expressed as percentage of change against

528 control conditions). Our results at these higher contentrations (50 μM) do not correspond to the
529 results found at physiological dose (1 μM). Overall, this indicates that bioavailable metabolites
530 from chlorogenic acid are unlikely to produce an *in vivo* direct FMO3 enzyme inhibition.
531
532 Through the *in vitro* approaches in this manuscript, we demonstrated that HepG2 and Hepa-1 cell
533 models are not a good model to study the inhibition of FMO3 activity by phenolic metabolites.
534 This was a result of a lack of production of TMAO in these two hepatic models, attribiuted to the
535 lack of FMO3 protein or its activity. However, we developed a fast screening method to evaluate
536 a direct FMO3 enzyme inhibition by bioavailable phenolic metabolies in rat hepatic microsomes,
537 with a detectable content of FMO3 that presented enzymatic activity. In conclusion, our results
538 show that bioavailable metabolites of chlorogenic acid do not have a strong inhibition potential on
539 the second step of TMAO formation. Rather, some minor inhibitory effects were reported for some
540 metabolites. Of note, even a modest inhibition of hepatic FMO3 could complement the inhibition
541 of TMA production by the microbiome *in vivo*. Overall, the lack of viable cell models to study
542 TMAO production highlights the need of *In vivo* experiments to elucidate if different treatments
543 (chlorogenic acid) are able to contribute to TMAO formation inhibition to mechanisms involving
544 FMO3 (*i.e*., downregulation of gene expression and/or protein content).
545
546 **6. References:**


547 1. World Health Organization (WHO) Cardiovascular Diseases Available online: https://www.who.int/.
548 2. Yang, S.; Li, X.; Yang, F.; Zhao, R.; Pan, X.; Liang, J.; Tian, L.; Li, X.; Liu, L.; Xing, Y.; et al. Gut
549 Microbiota-Dependent Marker TMAO in Promoting Cardiovascular Disease: Inflammation
550 Mechanism, Clinical Prognostic, and Potential as a Therapeutic Target. *Frontiers in Pharmacology*
551 **2019**, *10*, 1–14, doi:10.3389/fphar.2019.01360.
552 3. Randrianarisoa, E.; Lehn-Stefan, A.; Wang, X.; Hoene, M.; Peter, A.; Heinzmann, S.S.; Zhao, X.;
553 Königsrainer, I.; Königsrainer, A.; Balletshofer, B.; et al. Relationship of Serum Trimethylamine N-
554 Oxide (TMAO) Levels with Early Atherosclerosis in Humans. *Scientific Reports* **2016**, *6*, 1–9,
555 doi:10.1038/srep26745.
556 4. Yao, M.E.; Liao, P. Da; Zhao, X.J.; Wang, L. Trimethylamine-N-Oxide Has Prognostic Value in
557 Coronary Heart Disease: A Meta-Analysis and Dose-Response Analysis. *BMC Cardiovascular*
558 *Disorders* **2020**, *20*, 1–9, doi:10.1186/s12872-019-01310-5.
559 5. Rath, S.; Heidrich, B.; Pieper, D.H.; Vital, M. Uncovering the Trimethylamine-Producing Bacteria of
560 the Human Gut Microbiota. *Microbiome* **2017**, *5*, 1–14, doi:10.1186/S40168-017-0271-9.
561 6. Craciun, S.; Balskus, E.P. Microbial Conversion of Choline to Trimethylamine Requires a Glycyl
562 Radical Enzyme. *Proceedings of the National Academy of Sciences of the United States of America*
563 **2012**, *109*, 21307–21312, doi:10.1073/pnas.1215689109.

564 7. Iglesias-Carres, L.; Hughes, M.D.; Steele, C.N.; Ponder, M.A.; Davy, K.P.; Neilson, A.P. Use of
565 Dietary Phytochemicals for Inhibition of Trimethylamine N-Oxide Formation. *Journal of Nutritional*
566 *Biochemistry* **2021**, *91*, 108600, doi:10.1016/j.jnutbio.2021.108600.
567 8. Lang, D.H.; Yeung, C.K.; Peter, R.M.; Ibarra, C.; Gasser, R.; Itagaki, K.; Philpot, R.M.; Rettie, A.E.
568 Isoform Specificity of Trimethylamine N-Oxygenation by Human Flavin-Containing Monooxygenase
569 (FMO) and P450 Enzymes Selective Catalysis by Fmo3. *Biochemical Pharmacology* **1998**, *56*, 1005–
570 1012, doi:10.1016/S0006-2952(98)00218-4.
571 9. Zhang, J.; Cashman, J.R. Quantitative Analysis of FMO Gene MRNA Levels in Human Tissues. *Drug*
572 *Metabolism and Disposition* **2006**, *34*, 19–26, doi:10.1124/dmd.105.006171.
573 10. Bennett, B.J.; Vallim, T.Q.D.A.; Wang, Z.; Shih, D.M.; Meng, Y.; Gregory, J.; Allayee, H.; Lee, R.;
574 Graham, M.; Crooke, R.; et al. Trimethylamine-N-Oxide, a Metabolite Associated with
575 Atherosclerosis, Exhibits Complex Genetic and Dietary Regulation. *Cell Metabolism* **2013**, *17*, 49–60,
576 doi:10.1016/j.cmet.2012.12.011.
577 11. Subramaniam, S.; Fletcher, C. Trimethylamine N-Oxide: Breathe New Life. *British Journal of*
578 *Pharmacology* **2018**, *175*, 1344–1353, doi:10.1111/bph.13959.
579 12. Guan, R.; Van Le, Q.; Yang, H.; Zhang, D.; Gu, H.; Yang, Y.; Sonne, C.; Lam, S.S.; Zhong, J.;
580 Jianguang, Z.; et al. A Review of Dietary Phytochemicals and Their Relation to Oxidative Stress and
581 Human Diseases. *Chemosphere* **2021**, *271*, 129499, doi:10.1016/j.chemosphere.2020.129499.
582 13. Lutz, M.; Fuentes, E.; Ávila, F.; Alarcón, M.; Palomo, I. Roles of Phenolic Compounds in the
583 Reduction of Risk Factors of Cardiovascular Diseases. *Molecules* **2019**, *24*, 1–15,
584 doi:10.3390/molecules24020366.
585 14. Lu, H.; Tian, Z.; Cui, Y.; Liu, Z.; Ma, X. Chlorogenic Acid: A Comprehensive Review of the Dietary
586 Sources, Processing Effects, Bioavailability, Beneficial Properties, Mechanisms of Action, and Future
587 Directions. *Comprehensive Reviews in Food Science and Food Safety* **2020**, *19*, 3130–3158,
588 doi:10.1111/1541-4337.12620.
589 15. Iglesias-Carres, L.; Essenmacher, L.A.; Racine, K.C.; Neilson, A.P. Development of a High
590 Throughput Method to Study the Inhibitory Effect of Phytochemicals on Trimethylamine Formation.
591 *Nutrients* **2021**, *13*, 1466, doi:10.3390/nu13051466.
592 16. Iglesias-Carres, L.; Krueger, E.S.; Herring, J.A.; Tessem, J.S.; Neilson, A.P. Potential of Phenolic
593 Compounds and Their Gut Microbiota-Derived Metabolites to Reduce TMA Formation: Application of
594 an In Vitro Fermentation High-Throughput Screening Model. *Journal of Agricultural and Food*
595 *Chemistry* **2022**, *70*, 3207–3218, doi:10.1021/acs.jafc.2c00247.
596 17. Iglesias-carres, L.; Racine, K.C.; Neilson, A.P. Phenolic-Rich Beverages Reduce Bacterial TMA
597 Formation in an Ex Vivo-in Vitro Colonic Fermentation. *ChemRxiv.* **2022**, doi:10.26434/chemrxiv-
598 2022-f5vj6.
599 18. Zhang, X.; Shi, L.; Chen, R.; Zhao, Y.; Ren, D.; Yang, X. Chlorogenic Acid Inhibits Trimethylamine- N
600 -Oxide Formation and Remodels Intestinal Microbiota to Alleviate Liver Dysfunction in High l -
601 Carnitine Feeding Mice. *Food & Function* **2021**, *12*, 10500–10511, doi:10.1039/d1fo01778k.
602 19. Cosme, P.; Rodríguez, A.B.; Espino, J.; Garrido, M. Plant Phenolics: Bioavailability as a Key
603 Determinant of Their Potential Health-Promoting Applications. *Antioxidants* **2020**, *9*, 1–20,
604 doi:10.3390/antiox9121263.

605 20. Catalkaya, G.; Venema, K.; Lucini, L.; Rocchetti, G.; Delmas, D.; Daglia, M.; De Filippis, A.; Xiao, H.;
606 Quiles, J.L.; Xiao, J.; et al. Interaction of Dietary Polyphenols and Gut Microbiota: Microbial
607 Metabolism of Polyphenols, Influence on the Gut Microbiota, and Implications on Host Health. *Food*
608 *Frontiers* **2020**, *1*, 109–133, doi:10.1002/fft2.25.
609 21. Tomás-Barberán, F.A.; González-Sarrías, A.; García-Villalba, R.; Núñez-Sánchez, M.A.; Selma, M.
610 V.; García-Conesa, M.T.; Espín, J.C. Urolithins, the Rescue of "Old" Metabolites to Understand a
611 "New" Concept: Metabotypes as a Nexus among Phenolic Metabolism, Microbiota Dysbiosis, and
612 Host Health Status. *Molecular Nutrition and Food Research* **2017**, *61*, doi:10.1002/mnfr.201500901.
613 22. Bitner, B.F.; Ray, J.D.; Kener, K.B.; Herring, J.A.; Tueller, J.A.; Johnson, D.K.; Tellez Freitas, C.M.;
614 Fausnacht, D.W.; Allen, M.E.; Thomson, A.H.; et al. Common Gut Microbial Metabolites of Dietary
615 Flavonoids Exert Potent Protective Activities in β-Cells and Skeletal Muscle Cells. *Journal of*
616 *Nutritional Biochemistry* **2018**, *62*, 95–107, doi:10.1016/j.jnutbio.2018.09.004.
617 23. Álvarez-Cilleros, D.; Ramos, S.; Goya, L.; Martín, M.Á. Colonic Metabolites from Flavanols Stimulate
618 Nitric Oxide Production in Human Endothelial Cells and Protect against Oxidative Stress-Induced
619 Toxicity and Endothelial Dysfunction. *Food and Chemical Toxicology* **2018**, *115*, 88–97,
620 doi:10.1016/j.fct.2018.03.006.
621 24. Chen, P.Y.; Li, S.; Koh, Y.C.; Wu, J.C.; Yang, M.J.; Ho, C.T.; Pan, M.H. Oolong Tea Extract and
622 Citrus Peel Polymethoxyflavones Reduce Transformation of l -Carnitine to Trimethylamine- N-Oxide
623 and Decrease Vascular Inflammation in l -Carnitine Feeding Mice. *Journal of Agricultural and Food*
624 *Chemistry* **2019**, *67*, 7869–7879, doi:10.1021/acs.jafc.9b03092.
625 25. Koh, Y.C.; Li, S.; Chen, P.Y.; Wu, J.C.; Kalyanam, N.; Ho, C.T.; Pan, M.H. Prevention of Vascular
626 Inflammation by Pterostilbene via Trimethylamine-N-Oxide Reduction and Mechanism of Microbiota
627 Regulation. *Molecular Nutrition and Food Research* **2019**, *63*, 1–7, doi:10.1002/mnfr.201900514.
628 26. Shi, Y.; Hu, J.; Geng, J.; Hu, T.; Wang, B.; Yan, W.; Jiang, Y.; Li, J.; Liu, S. Berberine Treatment
629 Reduces Atherosclerosis by Mediating Gut Microbiota in ApoE-/- Mice. *Biomedicine and*
630 *Pharmacotherapy* **2018**, *107*, 1556–1563, doi:10.1016/j.biopha.2018.08.148.
631 27. Wu, T.; Gao, Y.; Hao, J.; Yin, J.; Li, W.; Geng, J.; Liu, R.; Sui, W.; Zhang, M. Lycopene, Amaranth,
632 and Sorghum Red Pigments Counteract Obesity and Modulate the Gut Microbiota in High-Fat Diet
633 Fed C57BL/6 Mice. *Journal of Functional Foods* **2019**, *60*, 103437, doi:10.1016/j.jff.2019.103437.
634 28. Wang, Z.; Roberts, A.B.; Buffa, J.A.; Levison, B.S.; Zhu, W.; Org, E.; Gu, X.; Huang, Y.; Zamanian-
635 Daryoush, M.; Culley, M.K.; et al. Non-Lethal Inhibition of Gut Microbial Trimethylamine Production
636 for the Treatment of Atherosclerosis. *Cell* **2015**, *163*, 1585–1595, doi:10.1016/j.cell.2015.11.055.
637 29. Zhou, P.; Zhao, X.N.; Ma, Y.Y.; Tang, T.J.; Wang, S.S.; Wang, L.; Huang, J.L. Virtual Screening
638 Analysis of Natural Flavonoids as Trimethylamine (TMA)-Lyase Inhibitors for Coronary Heart
639 Disease. *Journal of Food Biochemistry* **2022**, *00*, e14376, doi:10.1111/jfbc.14376.
640 30. Celius, T.; Pansoy, A.; Matthews, J.; Okey, A.B.; Henderson, M.C.; Krueger, S.K.; Williams, D.E.
641 Flavin-Containing Monooxygenase-3: Induction by 3-Methylcholanthrene and Complex Regulation by
642 Xenobiotic Chemicals in Hepatoma Cells and Mouse Liver. *Toxicology and Applied Pharmacology*
643 **2010**, *247*, 60–69, doi:10.1016/j.taap.2010.05.018.
644 31. Ripp, S.L.; Itagaki, K.; Philpot, R.M.; Elfarra, A.A. Species and Sex Differences in Expression of
645 Flavin-Containing Monooxygenase Form 3 in Liver and Kidney Microsomes. *Drug Metabolism and*
646 *Disposition* **1999**, *27*, 46–52.

647 32. Janmohamed, A.; Hernandez, D.; Phillips, I.R.; Shephard, E.A. Cell-, Tissue-, Sex- and
648 Developmental Stage-Specific Expression of Mouse Flavin-Containing Monooxygenases (Fmos).
649 *Biochem Pharmacol* **2004**, *68*, 73–83, doi:10.1016/j.bcp.2004.02.036.
650 33. Falls, J.G.; Ryu, D.Y.; Cao, Y.; Levi, P.E.; Hodgson, E. Regulation of Mouse Liver Flavin-Containing
651 Monooxygenases 1 and 3 by Sex Steroids. *Arch Biochem Biophys* **1997**, *342*, 212–223,
652 doi:10.1006/abbi.1997.9965.
653 34. Falls, J.G.; Blake, B.L.; Cao, Y.; Levi, P.E.; Hodgson, E. Gender Differences in Hepatic Expression of
654 Flavin-containing Monooxygenase Isoforms (FMO1, FMO3, and FMO5) in Mice. *J Biochem Toxicol*
655 **1995**, *10*, 171–177, doi:10.1002/jbt.2570100308.
656 35. Arzumanian, V.A.; Kiseleva, O.I.; Poverennaya, E. V. The Curious Case of the HepG2 Cell Line: 40
657 Years of Expertise. *International Journal of Molecular Sciences* **2021**, *22*,
658 doi:10.3390/ijms222313135.
659 36. Celius, T.; Pansoy, A.; Matthews, J.; Okey, A.B.; Henderson, M.C.; Krueger, S.K.; Williams, D.E.
660 Flavin-Containing Monooxygenase-3: Induction by 3- Methylcholanthrene and Complex Regulation
661 by Xenobiotic Chemicals in Hepatoma Cells and Mouse Liver. *Toxicol Appl Pharmacol.* **2010**, *247*,
662 60–69, doi:10.1016/j.taap.2010.05.018.
663 37. Fedejko-Kap, B.; Niemira, M.; Radominska-Pandya, A.; Mazerska, Z. Flavin Monooxygenases,
664 FMO1 and FMO3, Not Cytochrome P450 Isoenzymes, Contribute to Metabolism of Anti-Tumour
665 Triazoloacridinone, C-1305, in Liver Microsomes and HepG2 Cells. *Xenobiotica* **2011**, *41*, 1044–
666 1055, doi:10.3109/00498254.2011.604743.
667 38. Klick, D.E.; Shadley, J.D.; Hines, R.N. Differential Regulation of Human Hepatic Flavin Containing
668 Monooxygenase 3 (FMO3) by CCAAT/Enhancer-Binding Protein β (C/EBPβ) Liver Inhibitory and
669 Liver Activating Proteins. *Biochemical Pharmacology* **2008**, *76*, 268–278,
670 doi:10.1016/j.bcp.2008.05.002.
671 39. Klick, D.E.; Hines, R.N. Mechanisms Regulating Human FMO3 Transcription. *Drug Metabolism*
672 *Reviews* **2007**, *39*, 419–442, doi:10.1080/03602530701498612.
673 40. Farah, A.; Monteiro, M.; Donangelo, C.M.; Lafay, S. Chlorogenic Acids from Green Coffee Extract
674 Are Highly Bioavailable in Humans. *Journal of Nutrition* **2008**, *138*, 2309–2315,
675 doi:10.3945/jn.108.095554.
676 41. Hernandez, D.; Addou, S.; Lee, D.; Orengo, C.; Shephard, E.A.; Phillips, I.R. Trimethylaminuria and a
677 Human FMO3 Mutation Database. *Human Mutation* **2003**, *22*, 209–213, doi:10.1002/humu.10252.
678

679 ## 7. Figure Captions

680

681 **Figure 1:** Cell respiration rate (MTT assay) in HepG2 cells exposed to different concentration of TMA (0 – 200 μM) for
682 10 h (**A**), and HepG2 pre-treated with TMA 100 μM for 24 h and exposed to TMA 100 μM and different concentrations
683 of NADPH (0 – 2 mM) for 24 h (**B**). Results are expressed as percentage of change against control conditions ± SEM
684 ($n$=3). Different letters indicate statistically significant differences ($p$<0.05) by One-Way ANOVA (Tukey's *post hoc* test).

685

686 **Figure 2:** Lack of spontaneous (non cell-catalyzed) production of TMAO in HepG2 cell culture conditions for 24 h (**A**).
687 Lack of TMAO production in HepG2 cells pretreated with 100 μM TAM 24 h prior to treatment with TMA 100 μM and

688 different concentrations of NADPH (0 – 2 mM) for 24 h (**B**). Results are expressed as percentage of change against
689 control conditions ± SEM (*n*=3).
690
691 **Figure 3:** Lack of TMAO production in Hepa-1 cells. Effect of TMA concentration: Hepa-1 cells pre-treated with 100
692 μM TMA for 24 h, and then co-cultured with TMA 0 – 100 μM and NADPH 1 mM in MEM-α (**A**). Effect of NADPH
693 concentration: Hepa-1 cells pre-treated with 100 μM TMA for 24 h, and then co-cultured with NADPH 0 – 2 mM and
694 TMA 50 μM in MEM-α (**B**). Effect of media: MEM-α and complete (whole) growth media in pre-treated (TMA 100 μM
695 for 24 h) or un-pretreated Hepa-1 cells co-treated with TAM 50 μM and NADPH 1 mM (**C**). Background refers to
696 treatments without TMA and NADPH. Results are expressed as mean ± SEM (*n*=3). TMAO levels were not detected
697 (n.d.) throughout these experimental conditions.
698
699 **Figure 4**: Method validation for TMA and TMAO production and stability in microsome assay. Results are expressed
700 as mean μM ± SEM (*n*=3).
701
702 **Figure 5**: Kinetics of TMA consumption and TMAO production in microsome assay (33 μL/mL) with NADPH 1 mM and
703 TMA 0 μM (**A**), 20 μM (**B**) and 50 μM (**C**). Results are expressed as mean μM ± SEM (*n*=3).
704
705 **Figure 6:** Effect of different concentrations of methimazole (MTM) on TMA consumption (**A**) and TMAO production (**B**)
706 in microsome assay. Results are expressed as mean μM ± SEM (*n*=3). Background corresponds to no TMA or MTM
707 added in the reaction mix. Treatments not sharing common letters (to the right of the legend) have statistically different
708 ($p<0.05$) main effect of treatment by Two-Way ANOVA (Tukey's *post hoc* test).
709
710 **Figure 7:** Effect of chlorogenic acid-related compounds (1 μM) in the kinetic curves of TMA (**A**) and TMAO (**B**), as well
711 as the areas under the curve of TMA (**C**) and TMAO (**D**). Results are expressed as mean ± SEM (*n*=3). * indicates
712 statistical differences ($p<0.05$) in the levels of TMA or TMAO against control by Two-Way ANOVA (**A** & **B**) and by One-
713 Way ANOVA (**C** & **D**) (all by Dunnetts's *post hoc* test).
714
715 **Figure 8:** FMO3 levels in HepG2 and Hepa-1 (with and without pre-treatment with TMA 50μM and NADPH 0.2 mM for
716 24 h) and microsomes (not pre-treated). Results are expressed as ng FMO3 per mg protein ± SEM (*n*=3). Note that
717 the ELISA assay kit employed varied by species: mouse-specific FMO3 (kit MBS9327471) for Hepa-1 cells, rat-specific
718 FMO3 (kit MBS9901107) for rat microsomes, and human-specific FMO3 (MBS9901102) for HepG2 cells.
719

## Figure 1

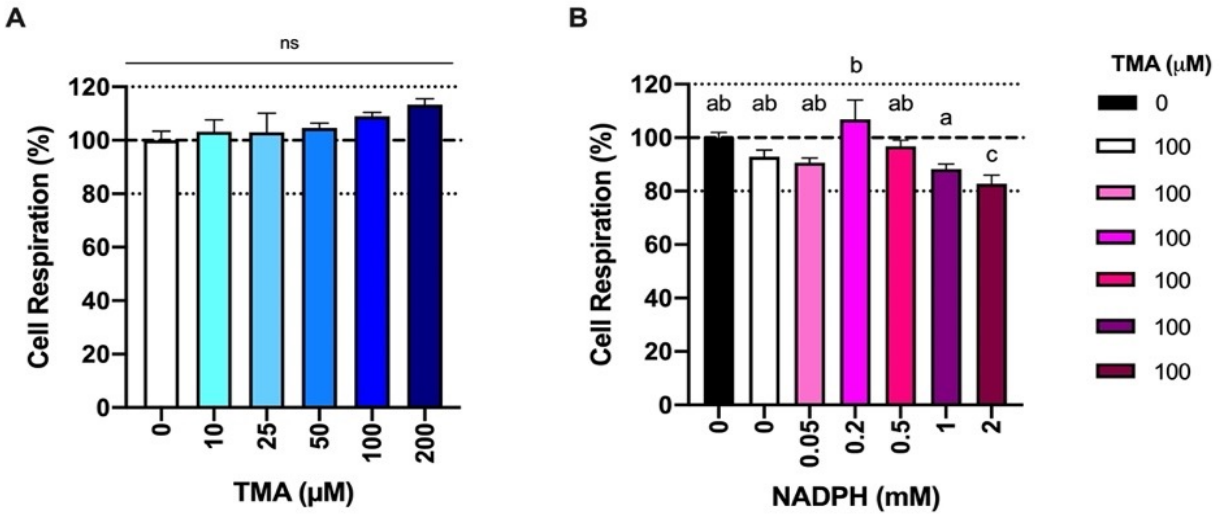


720 **Figure 1:** Cell respiration rate (MTT assay) in HepG2 cells exposed to different concentration of TMA (0 – 200 µM) for 10 h (**A**),
721 and HepG2 pre-treated with TMA 100 µM for 24 h and exposed to TMA 100 µM and different concentrations of NADPH (0 – 2
722 mM) for 24 h (**B**). Results are expressed as percentage of change against control conditions ± SEM (*n*=3). Different letters indicate
723 statistically significant differences ($p<0.05$) by One-Way ANOVA (Tukey's *post hoc* test).

## Figure 2

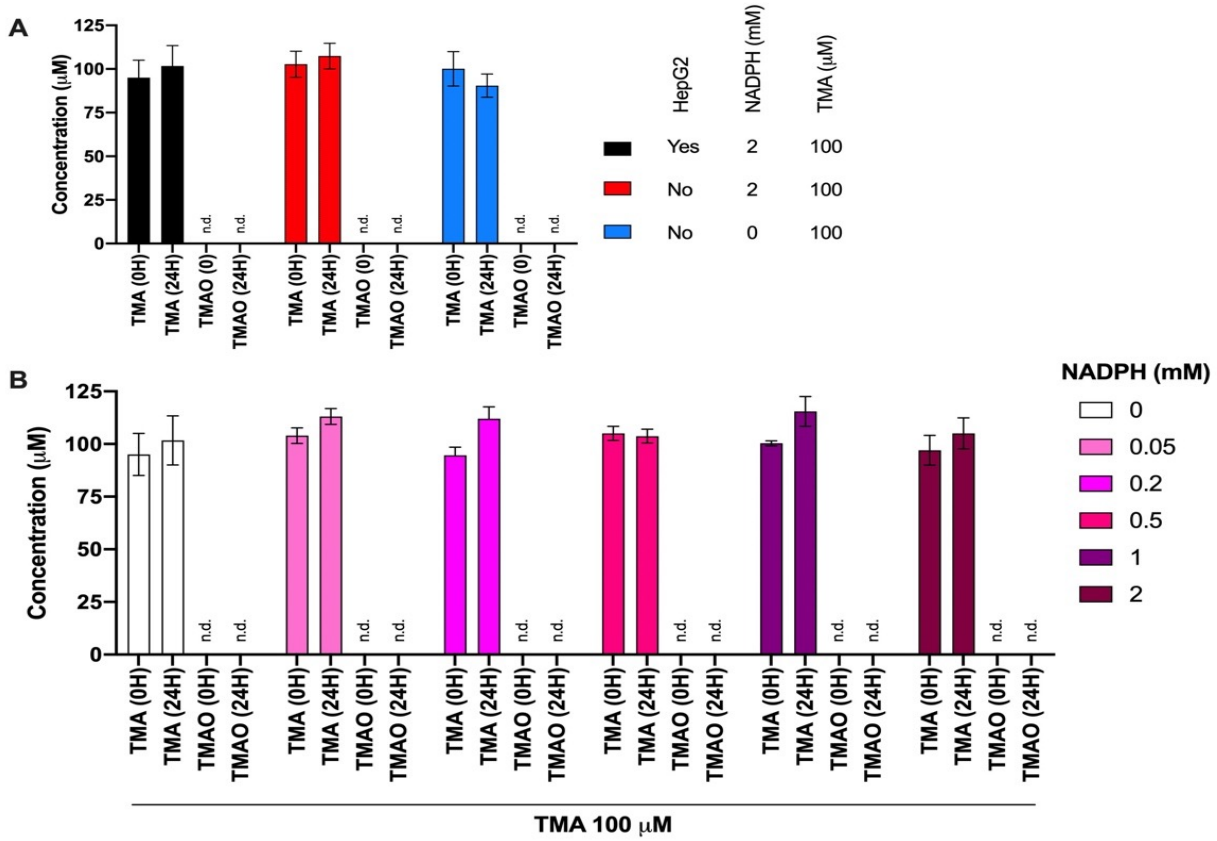


**Figure 2:** Lack of spontaneous (non cell-catalyzed) production of TMAO in HepG2 cell culture conditions for 24 h (**A**). Lack of TMAO production in HepG2 cells pretreated with 100 μM TAM 24 h prior to treatment with TMA 100 μM and different concentrations of NADPH (0 – 2 mM) for 24 h (**B**). Results are expressed as percentage of change against control conditions ± SEM (*n*=3).

## Figure 3

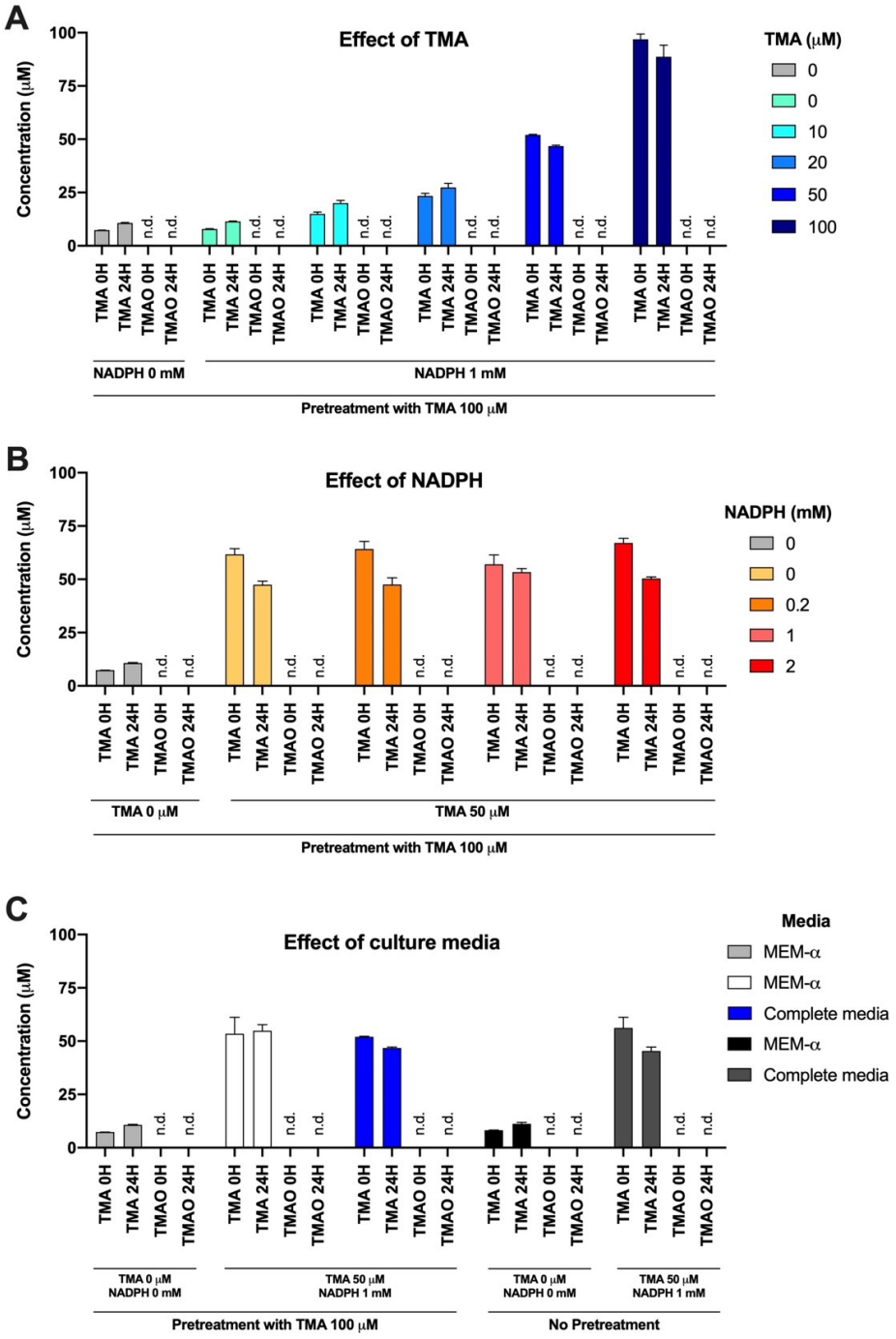


**Figure 3:** Lack of TMAO production in Hepa-1 cells. Effect of TMA concentration: Hepa-1 cells pre-treated with 100 μM TMA for 24 h, and then co-cultured with TMA 0 – 100 μM and NADPH 1 mM in MEM-α (**A**). Effect of NADPH concentration: Hepa-1 cells pre-treated with 100 μM TMA for 24 h, and then co-cultured with NADPH 0 – 2 mM and TMA 50 μM in MEM-α (**B**). Effect of media: MEM-α and complete (whole) growth media in pre-treated (TMA 100 μM for 24 h) or un-pretreated Hepa-1 cells co-treated with TAM 50 μM and NADPH 1 mM (**C**). Background refers to treatments without TMA and NADPH. Results are expressed as mean ± SEM (*n*=3). TMAO levels were not detected (n.d.) throughout these experimental conditions.

## Figure 4

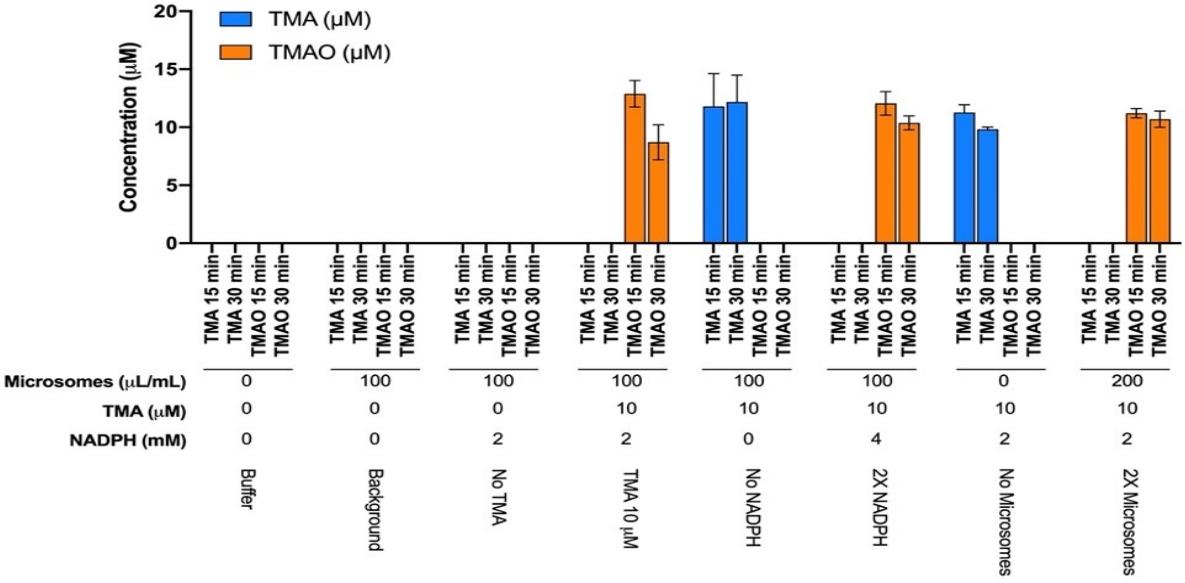


**Figure 4**: Method validation for TMA and TMAO production and stability in microsome assay. Results are expressed as mean μM ± SEM (*n*=3).

## Figure 5

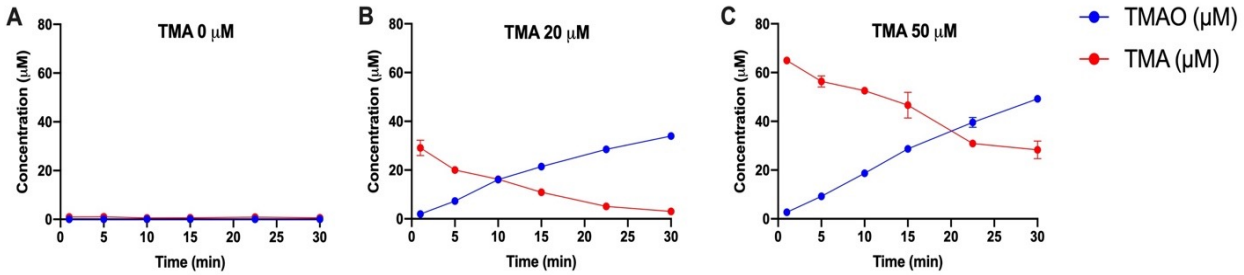


**Figure 5**: Kinetics of TMA consumption and TMAO production in microsome assay (33 μL/mL) with NADPH 1 mM and TMA 0 μM (**A**), 20 μM (**B**) and 50 μM (**C**). Results are expressed as mean μM ± SEM (*n*=3).

## Figure 6

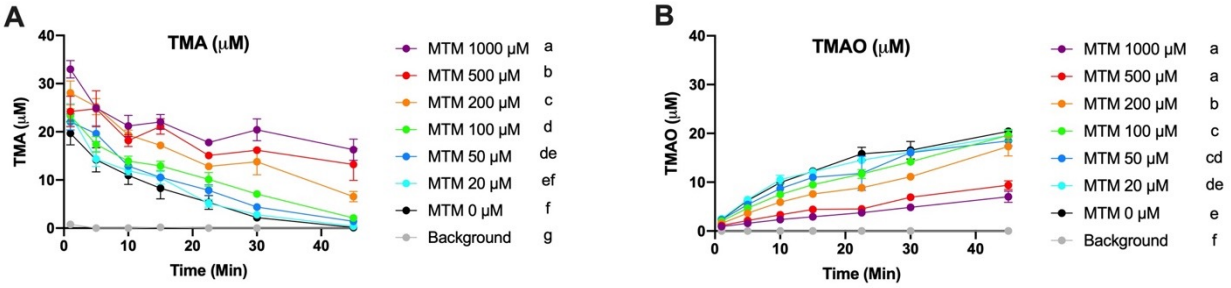


**Figure 6:** Effect of different concentrations of methimazole (MTM) on TMA consumption (**A**) and TMAO production (**B**) in microsome assay. Results are expressed as mean µM ± SEM (*n*=3). Background corresponds to no TMA or MTM added in the reaction mix. Treatments not sharing common letters (to the right of the legend) have statistically different ($p<0.05$) main effect of treatment by Two-Way ANOVA (Tukey's *post hoc* test).

## Figure 7

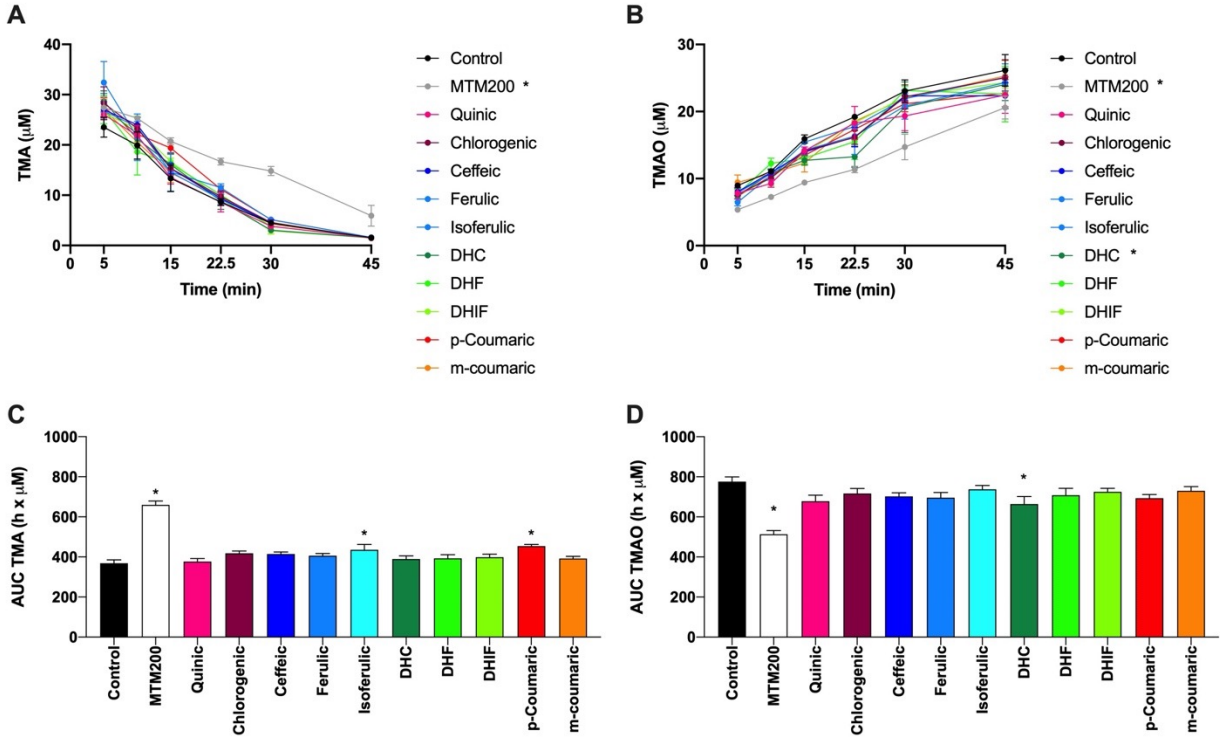


**Figure 7:** Effect of chlorogenic acid-related compounds (1 µM) in the kinetic curves of TMA (**A**) and TMAO (**B**), as well as the areas under the curve of TMA (**C**) and TMAO (**D**). Results are expressed as mean ± SEM (*n*=3). * indicates statistical differences ($p<0.05$) in the levels of TMA or TMAO against control by Two-Way ANOVA (**A** & **B**) and by One-Way ANOVA (**C** & **D**) (all by Dunnetts's *post hoc* test).

**Figure 8**

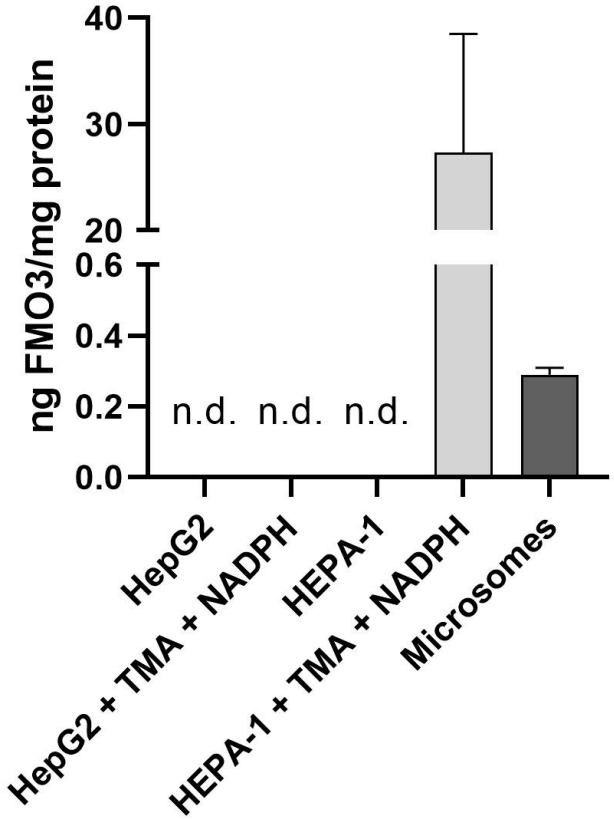


**Figure 8:** FMO3 levels in HepG2 and Hepa-1 (with and without pre-treatment with TMA 50µM and NADPH 0.2 mM for 24 h) and microsomes (not pre-treated). Results are expressed as ng FMO3 per mg protein ± SEM (*n*=3). Note that the ELISA assay kit employed varied by species: mouse-specific FMO3 (kit MBS9327471) for Hepa-1 cells, rat-specific FMO3 (kit MBS9901107) for rat microsomes, and human-specific FMO3 (MBS9901102) for HepG2 cells.